Chapter 16
Primary, Non-rechargeable Batteries

16.1 Introduction

Except for the discussions of the lithium/iodine cell in Chap. 10, all of the discussion concerning batteries for energy storage has been oriented toward understanding the properties of individual cell components and systems. The emphasis has been upon those that are most interesting for use in rechargeable batteries.

There are, however, a number of types of batteries that are very common and important, even though they cannot be readily recharged. They are often called primary batteries, and are typically discarded when they become discharged. Several of these will be discussed in this chapter.

Because some primary cells have higher values of specific energy than current rechargeable systems, there is continual interest in finding methods to electrically recharge them, rather than having to refurbish them chemically by reprocessing one or more of their components.

16.2 The Common Zn/MnO_2 "Alkaline" Cell

16.2.1 Introduction

Elemental zinc is used as the negative electrode in a number of aqueous electrolyte batteries. The most prominent example is the very common Zn/MnO_2 primary "alkaline cell" that is used in a wide variety of small electronic devices. Elemental zinc is the negative electrode reactant, MnO_2 the positive reactant, and the electrolyte is a solution of KOH. These cells are available in great numbers in standard AA and AAA sizes.

R.A. Huggins, *Energy Storage*, DOI 10.1007/978-3-319-21239-5_16

As will be discussed later, the positive electrode reaction in this case involves the insertion of hydrogen into the MnO_2 crystal structure, forming H_xMnO_2. A discussion of Zn/MnO_2 technology can be found in [1].

The initial open circuit voltage of these cells is in the range 1.5–1.6 V. This is greater than the decomposition voltage of water, which can be calculated from its Gibbs free energy of formation, 237.1 kJ/mol, to be 1.23 V at ambient temperatures from

$$\Delta E = -\left(\frac{\Delta G_f^*(H_2O)}{2F}\right) \tag{16.1}$$

It will be shown here that this is possible because the zinc negative electrode is covered by a thin layer of ionically conducting ZnO, the thermodynamic result is that its potential is several hundred millivolts lower than the potential at which gaseous hydrogen is normally expected to evolve if an unoxidized metal electrode were to be in contact with water.

The open circuit voltage decreases as energy is extracted and the residual capacity becomes reduced. This reduction in cell voltage is due to the change of the potential of the MnO_2 positive electrode due to the insertion of protons from the electrolyte. This can be described as changing the value of x in the composition H_xMnO_2 from zero to about 1. The proton content can be increased until the value of x becomes 2. However, as will be shown later, the second proton reaction occurs at a cell voltage of about 1 V, which is too low to be of practical use.

16.2.2 Thermodynamic Relationships in the H-Zn-O System

The potential and stability of the zinc electrode can be understood by consideration of the thermodynamics of the ternary H-Zn-O system, and its representation in a ternary phase stability diagram.

In addition to the elements and water, the only other relevant phase in this system is ZnO, and the value of its Gibbs free energy of formation is −320.5 kJ/mol at 25 °C.

As discussed earlier, one can use the values of the Gibbs free energy of formation of the different phases to determine which tie lines are stable in a ternary phase stability diagram. In this case the only possibilities would be either a line between Zn and H_2O or a line between ZnO and hydrogen. Because the Gibbs free energy of formation of ZnO is more negative than that of water, the second of these possible tie lines must be the more stable. The simple result in this case is shown in Fig. 16.1. It shows that a sub-triangle is formed that has Zn, ZnO, and H_2 at its corners. Another has water, ZnO, and hydrogen at its corners. The potentials of all compositions in the first triangle with respect to oxygen can be calculated from the Gibbs free energy change related to the simple binary reaction along its edge,

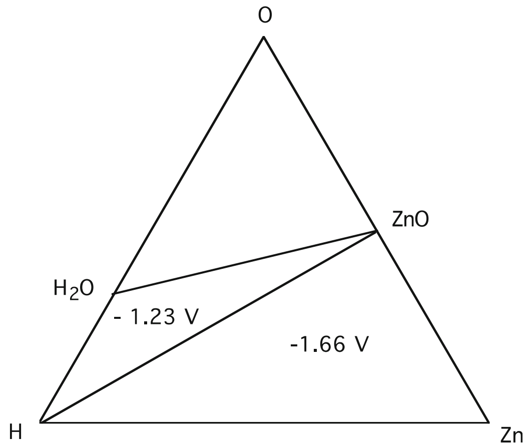

Fig. 16.1 Ternary phase stability diagram for the H-Zn-O system. The numbers within the ternary sub-triangles are the potentials relative to pure oxygen

$$Zn + {}^{1}\!/_{2}O_2 = ZnO \tag{16.2}$$

and the result is -1.66 V. The potential of all compositions in the second triangle is likewise related to the Gibbs free energy of formation of water, or -1.23 V relative to pure oxygen. That means that zinc has a potential that is 0.43 V more negative than the potential of pure hydrogen in aqueous electrolytes.

Because of the presence of the thin ionically conducting, but electronically insulating, layer of ZnO, water is not present at the electrochemical interface, the location of the transition between ionic conduction and electronic conduction, and hydrogen gas is not formed on the zinc. Thus the effective stability range of the electrolyte is extended, as discussed later.

16.2.3 Problems with the Zinc Electrode

Whereas its low potential is very attractive, there are two negative features of the use of zinc electrodes in aqueous systems. Both relate to its rechargeability in basic aqueous electrolytes.

One of these is that ZnO dissolves in KOH electrolytes, producing an appreciable concentration of zincate ions, $Zn(OH)_4{}^{2-}$, in which the Zn^{2+} cations are tetrahedrally surrounded by four OH^- groups. Nonuniform zincate composition gradients during recharging, as well as the ZnO on the surface, lead to the formation of *protrusions*, *filaments*, and *dendrites* during the re-deposition of zinc from the electrolyte at appreciable currents.

The other is that the zinc has a tendency to not redeposit upon the electrode at the same locations during charging of the cell as those from which it was removed during discharge. Gravitational de-mixing causes the concentration of zincate ions to increase at lower locations, leading to slight differences in the electrolyte conductivity. The result is that there is a gradual redistribution of the zinc, so that the lower portions of the electrode become somewhat thicker or denser as it is discharged and recharged. This effect is often called *shape-change*.

MnO_2 is polymorphic, which means that it can exist with a number of different crystal structures. It has been known for many years that they exhibit very different electrochemical behavior. The form found in mineral deposits has the rutile (beta) structure, and is called pyrolusite. It is relatively inactive as a positive electrode reactant in KOH electrolytes. It can be given various chemical treatments to make it more reactive, however. One of these produces a modification containing some additional cations that is called birnessite. Manganese dioxide can also be produced chemically, and then generally has the delta structure. The material that is currently much more widely used in batteries is produced electrolytically, and is called EMD. It has the gamma (ramsdellite) structure.

The reason for the differences in the electrochemical behavior of the several morphological forms of manganese dioxide presented a quandary for a number of years. It was known, however, that the gamma electrochemically active materials contain about 4 % water in their structures that can be removed by heating to elevated temperatures (100–400 °C), but the location and form of that water remained a mystery. This problem was solved by Ruetschi, who introduced a cation vacancy model for MnO_2 [2, 3].

The basic crystal structure of the various forms of MnO_2 contains Mn^{4+} ions in octahedral holes within hexagonally (almost) close-packed layers of oxide ions. That means that each Mn^{4+} ion has six oxygen neighbors, and these MnO_6 octahedra are arranged in the structure to share edges and corners. Differences in the edge- and corner-sharing arrangements result in the various polymorphic structures mentioned above.

If some of the Mn^{4+} ions are missing (cation vacancies are present), their missing positive charge has to be compensated by something else in the crystal structure. The Ruetschi model proposed that this charge balance is accomplished by the local presence of four protons. These protons would be bound to the neighboring oxide ions, forming a set of four OH^- ions. This local configuration is sometimes called a Ruetschi defect. There is very little volume change, as OH^- ions have essentially the same size as O_{2-} ions, and these species play the central role in determining the size of the crystal structure.

On the other hand, reduction of the MnO_2 occurs by the introduction of additional protons during discharge, as first proposed by Coleman [4], and does produce a volume change. The charge of these added mobile protons is balanced by a reduction in the charge of some of the manganese ions present from Mn^{4+} to Mn^{3+}. Mn^{3+} ions are larger than Mn^{4+} ions, and this change in volume during reduction has been observed experimentally.

The presence of protons (or OH^- ions) related to the manganese ion vacancies facilitates the transport of additional protons as the material is discharged. This is why these materials are very electrochemically reactive.

16.2.4 The Open Circuit Potential

The EMD is produced by oxidation of an aqueous solution of manganous sulfate at the positive electrode of an electrolytic cell. This means that the MnO_2 that is produced is in contact with water.

The phase relations, and the related ternary phase stability diagram, for the H-Mn-O system can be determined by use of available thermodynamic information [5, 6], as discussed in previous chapters. From this information it becomes obvious which neutral species reactions determine the potential ranges of the various phases present, and their values.

Following this approach, it is found that the lower end of the stability range of MnO_2 is at a potential that is 1.014 V vs. one atmosphere of H_2. The upper end is well above the potential at which oxygen evolves by the decomposition of water.

Under equilibrium conditions all oxides exist over a range of chemical composition, being more metal-rich at lower potentials, and more oxygen-rich at higher potentials. In the higher potential case, an increased oxygen content can result from either the presence of cation (Mn) vacancies or oxygen interstitials. In materials with the rutile, and related, structures that have close-packed oxygen lattices the excess energy involved in the formation of interstitial oxygens is much greater than that for the formation of cation vacancies. As a result, it is quite reasonable to assume that cation vacancies are present in the EMD MnO_2 that is formed at the positive electrode during electrolysis.

Due to the current that flows during the electrolytic process the potential of the MnO_2 that is formed is actually higher than the equilibrium potential for the decomposition of water. A number of other oxides with potentials above the stability range of water have been shown to oxidize water. Oxygen gas is evolved, and they become reduced by the insertion or protons. Therefore, it is quite reasonable to expect that EMD MnO_2 would have Mn vacancies, and that there would also be protons present, as discussed by Ruetschi [2, 3].

When such positive oxides oxidize water and absorb hydrogen as protons and electrons, their potentials decrease to the oxidation limit of water, 1.23 V vs. H_2 at 25 °C. This is the experimentally observed value of the open circuit potential of MnO_2 electrodes in Zn/MnO_2 cells.

This water oxidation phenomenon that results in the insertion of protons into MnO_2 is different from the insertion of protons by the absorption of water into the crystal structure of materials that initially contain oxygen vacancies, originally discussed by Stotz and Wagner [7]. It has been shown that both mechanisms can be present in some materials [8, 9].

16.2.5 Variation of the Potential During Discharge

As mentioned above, this electrode operates by the addition of protons into its crystal structure. This is a single-phase insertion reaction, and therefore the potential varies with the composition, as discussed earlier.

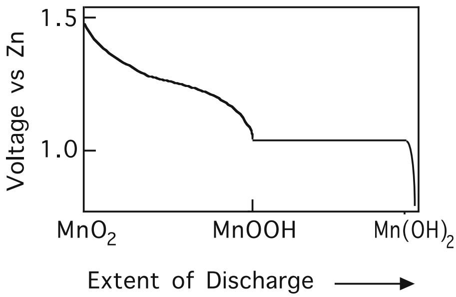

Fig. 16.2 Schematic discharge curve of Zn/MnO_2 cell

If all of the initially present Mn^{4+} ions are converted to Mn^{3+} ions, the overall composition can be expressed as $HMnO_2$, or MnOOH.

It is also possible to introduce further protons, so that the composition moves in the direction of $Mn(OH)_2$. In this case, however, there is a significant change in the crystal structure, so that the mechanism involves the translation of a two-phase interface between MnOOH and $Mn(OH)_2$. This is analogous to the main reaction involved in the operation of the nickel electrode, as will be discussed later.

The sequence of these two types of reactions during discharge of a MnO_2 electrode is illustrated in Fig. 16.2.

The second, two-phase, reaction occurs at such a low cell voltage that the energy that is available is generally not used. Such cells are normally considered to only be useful down to about 1.2 V.

Although these Zn/MnO_2 cells are generally considered to be non-rechargeable, there have been some developments that make it possible to recharge them a modest number of times, and a small fraction of the alkaline cell market has been oriented in this direction. This involves modifications in the design and proprietary changes in the composition of the materials. Their rechargeability depends upon the depth to which they have been discharged, and there is a gradual reduction in the available capacity.

16.3 Ambient Temperature Li/FeS_2 Cells

Another type of consumer battery that is gradually becoming more popular in a number of consumer markets is the Li/FeS_2 cell. In this case the negative electrode is lithium metal. The electrolyte is a lithium salt dissolved in an organic solvent similar to that used in rechargeable lithium batteries.

The potential of the elemental lithium negative electrode is constant, but that of the positive electrode varies with the state of charge. At very low current drain, it shows two voltage plateaus, at about 1.7 V and 1.5 V versus lithium, as seen in Fig. 16.3. This indicates the formation of an intermediate phase, and therefore a sequence of two different reactions.

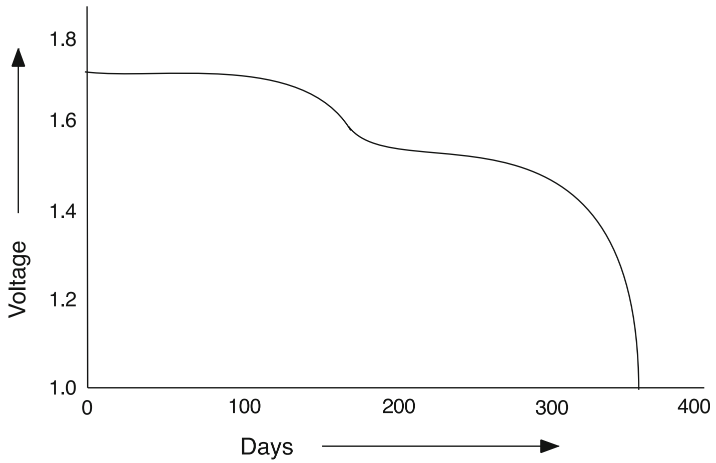

Fig. 16.3 Variation of the cell voltage with state of charge for Li/FeS_2 cells

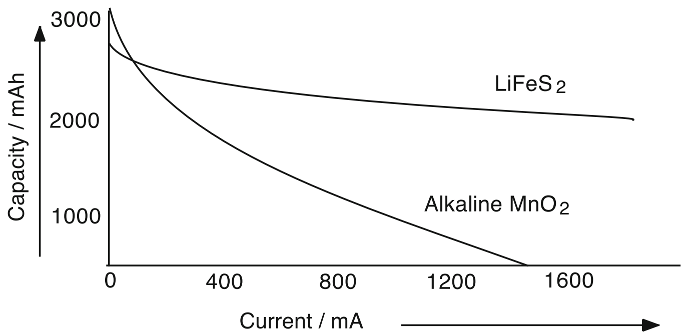

Fig. 16.4 Variation of the capacity of typical Li/FeS_2 cells with the current drain

At moderate, or greater, currents, the plateau structure disappears, and the output voltage drops steadily from about 1.6 to 1.5 V with the state of charge. This means that the intermediate phase does not form under those conditions.

The voltage of this type of battery is about 0.1 V higher than that of the common alkaline cells, and there is less fade as the cell becomes discharged. The primary advantage of the Li/FeS_2 cells over the less expensive Zn/MnO_2 cells is their ability to handle higher currents. This is shown in Fig. 16.4. This property makes them especially useful for pulse applications, such as in cameras.

16.4 Li/I_2 Batteries for Heart Pacemakers

There was a discussion of the non-rechargeable Li/I_2 batteries that are commonly used to provide power for heart pacemakers in Chap. 10. There is no need to repeat that material here, other than to point out the unusual situation that the reaction product, LiI, is actually the electrolyte in this case.

16.5 Lithium/Silver Vanadium Oxide Defibrillator Batteries

Another type of implantable primary cell that is now used to provide power for medical devices, such as defibrillators, is the lithium/silver vanadium oxide cell. The attractive features of this chemistry were first recognized in 1979 [10, 11]. The person responsible for the commercial development of these batteries, Esther Takeuchi, received the National Medal of Technology and Innovation from President Obama in October, 2009.

The negative electrode in these cells is elemental lithium, and the electrolyte is the lithium salt $LiBF_4$ in an organic solvent, propylene carbonate. The positive electrode starts as $AgV_2O_{5.5}$, a member of the family of electronically conducting oxides called vanadium bronzes [12].

Lithium reacts with this positive electrode material by an insertion reaction that can be written as

$$xLi + AgV_2O_{5.5} = Li_xAgV_2O_{5.5} \tag{16.3}$$

This reaction occurs over several steps, with corresponding values of x. This can be seen from the plot of the cell voltage as a function of the extent of this reaction shown in Fig. 16.5.

Charge balance is accomplished by a change in the effective charge of the cations originally in the vanadium bronze. In $AgV_2O_{5.5}$ all of the vanadium ions have an effective charge of 5+. Upon adding Li+ ions, the system moves into a constant-potential 2-phase regime, where both $AgV_2O_{5.5}$ and $LiAgV_2O_{5.5}$ are present. When the overall composition reaches the end of that voltage plateau, it moves into a variable-potential composition range in which only the phase $LiAgV_2O_{5.5}$ is present, and half of the vanadium ions have a charge of 5+, and the other half have a charge of 4+. The addition of 2 additional lithium ions causes the composition to move into another two-phase plateau in which the phase $LiAgV_2O_{5.5}$ is in equilibrium with a composition that is nominally $Li_3AgV_2O_{5.5}$. The effective charge of the vanadium ions in this latter phase is still 4+, but the nominal charge upon the silver ions has become zero. This means that there must be some particles of elemental silver present in the microstructure in addition to a phase of composition $Li_3V_2O_{5.5}$. Experiments have shown that the lower-lithium

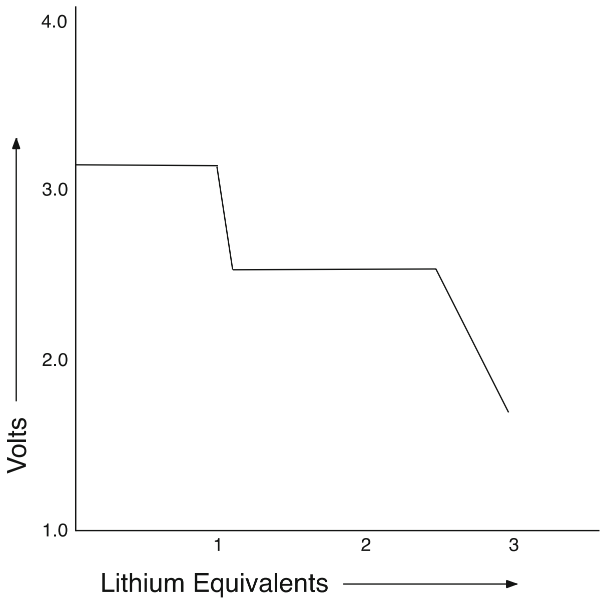

Fig. 16.5 Schematic illustration of the variation of the cell voltage as a function of the amount of lithium reacted

reactions are reversible, but the last, which involves the precipitation of a new phase, is not.

The decrease of voltage as the cell is discharged allows the state of charge to be readily determined by voltage measurements. This is important when such power sources are used in implantable medical devices. These cells exhibit a very low rate of self-discharge, have a long shelf life, and store a large amount of energy per unit volume, 930 Wh/l. The latter feature is attractive for applications in which battery size is important.

16.6 Zn/Air Cells

Primary cells based upon the reaction of zinc with air have been available commercially for a number of years. This chemistry can produce a rather large value of specific energy, is relatively inexpensive, and presents no significant environmental problems. One of the major applications is as a power source for small hearing aids.

A cell with metallic zinc as the negative electrode and oxygen (or air) on the positive side is shown schematically in Fig. 16.6.

There must be a mechanism for the flow of electrons into and out of an external electronic circuit from both electrodes. This is accomplished on the negative side by contact with metallic zinc. On the positive side there is a porous metallic conductor

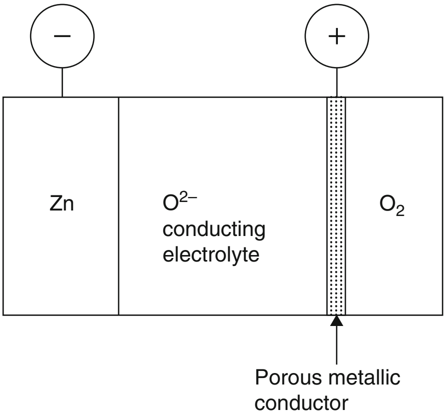

Fig. 16.6 Schematic representation of a Zn/O_2 cell

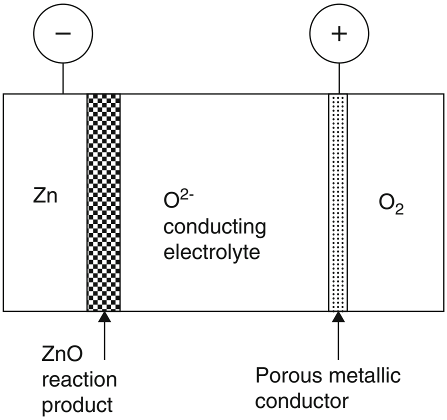

Fig. 16.7 Schematic representation of a Zn/O_2 cell that is partially discharged

in contact with both the oxygen reactant and the alkaline electrolyte. Although this metal plays no role in the overall cell reaction, the three-phase contact allows the electrochemical reaction that converts neutral atoms into ions and electrons.

The discharge reaction mechanism involves the transport of oxygen across the cell from the positive to the negative electrode, with the formation of ZnO on top of the Zn. A cell that is partially discharged is shown schematically in Fig. 16.7.

ZnO is an electronic conductor, so the electrochemical interface, where the electrical charge transport mechanism is converted from ions to electrons, is at the interface between the ZnO and the electrolyte. It is the electric potential at that interface that determines the externally measurable electrical potential of the negative electrode.

The reaction that determines the potential is generally assumed to be the formation of ZnO

$$Zn + {}^{1}\!/_{2}O_2 = ZnO \tag{16.4}$$

so that the voltage would be determined by the Gibbs free energy of formation of ZnO from zinc and oxygen.

$$E = \frac{\Delta G_f(\mathrm{ZnO})}{zF} \tag{16.5}$$

where $z = 2$, and F is the Faraday constant, 96.5 kJ/V equivalent. The value of ΔG_f(ZnO) at 298 K is 320.5 kJ/mol, so the equilibrium voltage E is 1.66 V at that temperature.

However, these cells operate in air, rather than pure oxygen. Therefore the chemical potential of oxygen is lower, and the electrical potential of the positive electrode is reduced. The chemical potential of oxygen in the positive electrode can be expressed as

$$\mu(\mathrm{O_2}) = \mu^0(\mathrm{O_2}) + RT\ln p(\mathrm{O_2}) \tag{16.6}$$

where $\mu^0(O_2)$ is the chemical potential of oxygen in its standard state, a pressure of 1 atm at the temperature in question, and $p(O_2)$ is the actual oxygen pressure at the electrode.

In air the oxygen partial pressure is approximately 0.21 atm, so that the cell voltage is reduced by

$$\Delta E = \frac{RT}{zF}\ln(0.21) \tag{16.7}$$

The result is that the equilibrium voltage of the Zn/O_2 cell when air is the reactant on the positive side should be reduced by 0.02 V. Thus a Zn/air cell should have an open circuit voltage of 1.64 V. If the oxygen pressure is maintained at a constant value, the voltage will be independent of the state of charge, i.e., will have the characteristics of an infinite plateau in a battery discharge curve.

The value of the maximum theoretical specific energy can be calculated from this information using the weights of the reactants. As discussed in Chap. 9, the value of the MTSE is given by

$$MTSE = 26,805\ \ (zE)/W_\mathrm{t} \quad \mathrm{Wh/kg} \tag{16.8}$$

The value of the reactant weight, W_t, is the weight of a mol of Zn (65.38 g) plus the weight of 1/2 mol of oxygen (8 g), or a total of 73.38 g per mol of reaction. The value of z is 2, the number of elementary charges involved in the virtual cell reaction.

Using this value and a cell voltage of 1.64 V for the case of air at the positive electrode, the MTSE is 1198 Wh/kg. If pure oxygen were used, it would be 1213 Wh/kg.

But there is a problem. The measured open circuit voltage of commercial Zn/air cells is about 1.5 V, not 1.64 V. The reason for this has to do, again, with what is actually going on at the positive electrode. The normal assumption is that the positive electrode reactant is oxygen, and therefore the potential should be that of pure oxygen at the partial pressure of air.

Experiments have shown the presence of peroxide ions at the positive electrode in alkaline aqueous cells. Instead of a conversion of oxygen from O_2 in the gas phase to O^{2-} ions in the electrolyte, there is an intermediate step, due to the presence of peroxide ions.

In peroxide ions, O^-, oxygen is at an intermediate charge state between neutral oxygen, O^0, in oxygen molecules in the gas, and oxide ions, O^{2-}, in the KOH electrolyte. In such aqueous systems this can be written as two steps in series

$$O_2 + H_2O + 2e^- = HO_2^- + OH^- \tag{16.9}$$

and

$$HO_2^- + H_2O + 2e^- = 3OH^- \tag{16.10}$$

The result is that the electrical potential in the positive electrode is determined by the presence of hydrogen peroxide, which is formed by the reaction of oxygen with the KOH electrolyte.

This is also the case with aqueous electrolyte hydrogen/oxygen fuel cells, where the open circuit voltage is determined by the presence of peroxide, rather than oxide, ions [13–15]. This is shown in Fig. 16.8. On the other hand, high temperature proton or oxide ion-conducting fuel cells have open circuit voltages that correspond to the assumption that the positive electrode reactant is oxygen.

Zn/O_2 cells are sold with a removable sealing material that prevents access of air to the positive electrode structure so that there is no self-discharge before they are used.

Their specific energy is very large, about 30 times the value of the maximum theoretical specific energy of a typical Pb/PbO_2 cell, so it is obvious why there is an interest in finding a way to make this system reversible. To do so, three general problems must be solved; the rechargeability of the zinc oxide product, the reversibility of the air electrode, and the sensitivity of the KOH electrolyte to contamination from CO_2 in the ambient air. CO_2 reacts with hydroxides to form solid carbonates, which can block the ionic transport through the electrolyte.

Development efforts toward the alleviation or avoidance of these problems have been undertaken in a number of laboratories, but they have not yet led to large-scale applications.

A large effort undertaken with the support of the German Post some years ago ran into several problems, the major one being the need for centralized chemical

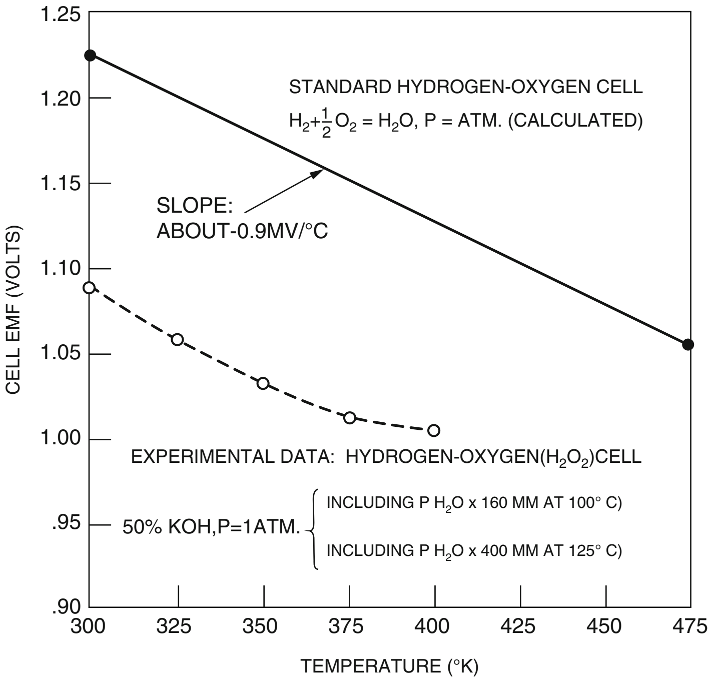

Fig. 16.8 Experimental data on the voltage of aqueous fuel cells, showing the influence of the presence of peroxide ions at the positive electrode. After [6]

regeneration of the zinc oxide product back into useful zinc electrodes. Transportation to and from such facilities can put a major load on rail or highway transportation systems.

16.7 Li/CF_x Cells

Lithium reacts with poly(carbon monofluoride), CF_x, at ambient temperatures.

The value of x in CF_x can vary from about 0.9 to 1.2, depending upon its synthesis parameters.

These cells are generally used in situations in which low to moderate rates are required.

Elemental lithium is used as the negative electrode reactant, and the electrolyte is typically a solution of $LiBF_4$ in propylene carbonate. The reactant in the positive electrode is powdered CF_x. Although this material has a lamellar structure that can be thought of as analogous to graphite, it actually consists of an infinite array of cyclohexane "boats" [16] instead of thin graphene sheets. Lithium does not readily move between these layers, and therefore the electrode reaction mechanism does not involve insertion, as in the case of lamellar graphite.

Instead, a polyphase reaction occurs during discharge that can be written as

$$xLi + CF_x = xLiF + C \tag{16.11}$$

Since this is a simple displacement reaction, the voltage remains constant, at 2.75 V, during discharge.

Because the reactants have low weights, the maximum theoretical specific energy, the MTSE, of these cells is very high, 1940 Wh/kg. This would be attractive for use for implantable medical applications. However, because the voltage remains constant, it is difficult to determine when the capacity is almost consumed. An indication that a power source is soon going to reach its end-of-life is especially important when it is used for such purposes, and this problem is currently receiving a considerable amount of attention.

16.8 Reserve Batteries

16.8.1 Introduction

The discussion of positive electrodes in lithium batteries thus far has assumed that the reactants are either solids or gases. However, this is not necessary, and there are two types of primary batteries that have been available commercially for a number of years in which the reactant is a liquid, the Li/SO_2 and $Li/SOCl_2$ (thionyl chloride) systems. They both have very high specific energies. But because of safety considerations they are not in general use, and are being produced primarily for military and space purposes.

These are examples of *reserve batteries*, in which some method is used to prevent their operation until the energy is needed. There are two general ways in which this can be done.

One is to prevent the electrolyte from contacting one or both of the electrodes. This prevents self-discharge as well as the operation of any unwanted side reactions. One way to do this is to contain the electrolyte in a glass container that can be broken when cell operation is desired. A second method involves the use of an electrolyte that does not conduct current until it melts at an elevated temperature. When battery operation is desired, the electrolyte is heated to above its melting point. Examples of both of these strategies are discussed below.

16.8.2 The Li/SO_2 System

These cells are generally constructed with large surface area carbon electrodes on the positive side, and x-ray experiments have shown that $Li_2S_2O_4$ is formed there upon discharge. The discharge curve is very flat, at 3.0 V, as shown in Fig. 16.9.

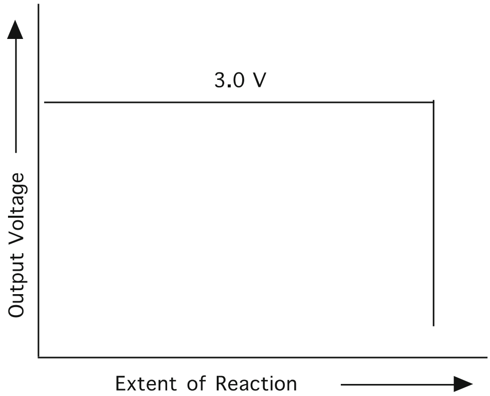

Fig. 16.9 Schematic discharge curve for a Li/SO_2 cell

Table 16.1 Gibbs free energies of formation of phases in the Li-S-O system at 25 °C

Phase	Gibbs free energy of formation (kJ/mol)
Li_2O	−562.1
SO_2	−300.1
Li_2S	−439.1
$Li_2S_2O_4$	−1179.2

As discussed earlier, this type of behavior indicates that the cell operates by a reconstitution reaction. It should be possible to calculate the voltage by consideration of the thermodynamic properties of the phases involved in this system at ambient temperature. These are shown in Table 16.1.

From this information the stable tie lines in the ternary phase stability diagram for this system can be determined, as described earlier. The reaction equations relevant to each of the sub-triangles can also be identified, and their potentials calculated. The resulting diagram is shown in Fig. 16.10.

It can be seen that the $Li_2S_2O_4$–SO_2–O sub-triangle has a potential of 3.0 V versus lithium. Since the SO_2–$Li_2S_2O_4$ tie line on the edge of that triangle points at the lithium corner, no oxygen is formed by the reaction of lithium with SO_2 to produce $Li_2S_2O_4$.

The formal reaction for this cell is therefore

$$2Li + 2SO_2 = Li_2S_2O_4 \tag{16.12}$$

The theoretical specific energy of this cell can be calculated to be 4080 kWh/kg, a high value.

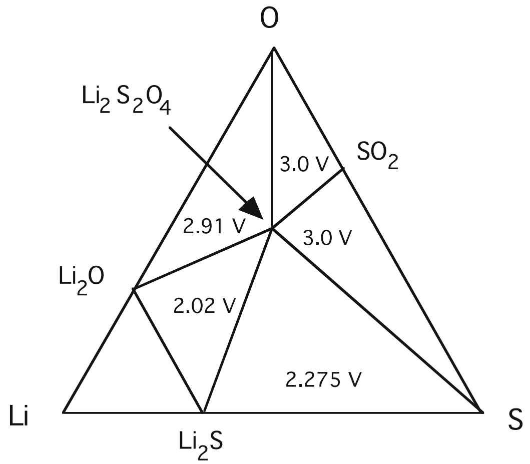

Fig. 16.10 Phase stability diagram for the ternary Li-S-O system at ambient temperature

16.8.3 The Li/SOCl$_2$ System

The lithium/thionyl batteries react at a somewhat higher constant voltage plateau, at 3.66 V.

The formal reaction is known to be

$$4Li + 2SOCl_2 = 4LiCl + S + SO_2 \tag{16.13}$$

This involves the Li-S-Cl-O quaternary system. In order to visualize the behavior of this system in a manner similar to that for the Li/SO_2 cell above, a tetrahedral figure would have to be drawn, and the constant voltage plateaus related to each of the sub-tetrahedra calculated. While straightforward, this is a bit too complicated to be included here, however.

The theoretical specific energy of this cell can be calculated to 7250 kWh/kg, which is a very high value.

16.8.4 Li/FeS$_2$ Elevated Temperature Batteries

A good deal of effort went into the development of a high temperature system that uses FeS_2 as the positive electrode reactant, but had either Li-Al or Li-Si alloys, rather than lithium metal, on the negative side. The electrolyte was a molten Li-K halide salt that has a eutectic temperature of 320 °C. These cells operated at temperatures over 400 °C, and the open circuit voltage was about 1.9 V, with most of the capacity obtained at 1.7 V. The initial development was aimed at their use to power electric vehicles, where their favorable high power operation is attractive. However, the appearance of other alternatives, such as ambient temperature lithium-ion systems, caused this work to be discontinued in the late 1990s.

Because the molten salt electrolyte is only conductive at elevated temperatures, such cells can be stored at ambient temperature and used as *reserve batteries*. Upon heating the electrolyte melts and the cell becomes operable. As mentioned above, this type of reserve batteries, often called *thermal batteries*, have been used for military applications in which a long shelf life is very important.

References

1. Scarr RF, Hunter JC, Slezak PJ (2002) Alkaline—Manganese Dioxide Batteries, in Handbook of Batteries, 3rd. edition, ed. D. Linden and T.B. Reddy, McGraw-Hill, p. 10.1
2. Ruetschi P (1984) J Electrochem Soc 131:2737
3. Ruetschi P, Giovanoli R (1988) J Electrochem Soc 135:2663
4. Coleman JJ (1946) Trans Electrochem Soc 90:545
5. Barin I (1995) Thermochemical Data of Pure Substances, 3rd edn. VCH, Weinheim, Published Online 24 Apr 2008. ISBN 9783527619829783527619825
6. Pourbaix M (1966) Atlas of Electrochemical Equilibria. Pergamon Press, Oxford, UK
7. Stotz S, Wagner C (1966) Ber Bunsenges Physik Chem 70; 781
8. Netz A, Chu WF, Thangadurai V, Huggins RA, Weppner W (1999) Ionics 5:426
9. Huggins RA (2006) J Power Sources 153:365
10. Liang CC, Boltser ME, Murphy RM (1982), US Patent 4,391,729
11. Liang CC, Boltser ME, Murphy RM (1982), US Patent 4,310,609
12. Takeuchi ES, Thiebolt WC III (1988) J Electrochem Soc 135:2691
13. Berl WG (1943) Trans Electrochem Soc 83:253
14. Winsel AW (1963) Advanced Energy Conversion, vol 3. Pergamon Press, Oxford
15. Kordesch KV, Berger C (1968) Handbook of Fuel Cell Technology. Prentice-Hall, Inc., New York, p 361
16. Ebert LB, Brauman JI, Huggins RA (1974) J Amer Chem Soc 96:7841